

Title	Local structures of amorphous (Ni _{0.6} Nb _{0.4}) _{100-x} Zr _x (x=30, 35, 40) alloys by XAFS
Author(s)	Matsuura, Makoto; Konno, Kazuya; Fukuhara, Mikio et al.
Citation	Transactions of JWRI. 2010, 39(2), p. 296-297
Version Type	VoR
URL	https://doi.org/10.18910/24836
rights	
Note	

Osaka University Knowledge Archive : OUKA

<https://ir.library.osaka-u.ac.jp/>

Osaka University

Local structures of amorphous $(\text{Ni}_{0.6}\text{Nb}_{0.4})_{100-x}\text{Zr}_x$ ($x=30, 35, 40$) alloys by XAFS[†]

MATSUURA Makoto *, KONNO Kazuya **, FUKUHARA Mikio *, FUJIMA Nobuhisa ***
and INOUE Akihisa ****

KEY WORDS: (XAFS) (Local structure) (Amorphous) (Metallic glass) (NiNbZr) (Icosahedral cluster)

1. Introduction

A wide composition range of amorphous-forming ability has been reported in the ternary Ni-Nb-Zr alloy system by Kimura *et al.* [1]. Because Zr and Nb have high hydrogen permeability, amorphous Ni-Nb-Zr alloys have been studied to develop superior hydrogen permeation materials. Atomic structure of the amorphous Ni-Nb-Zr(H) alloys has been studied Yamaura *et al.* [2]. and Sakurai *et al.* [3] by XRD and XAFS, respectively, in which the local structural change by hydrogen absorption was the main issue. Recently amorphous $(\text{Ni}_{0.6}\text{Nb}_{0.4})_{100-x}\text{Zr}_x$ ($x=30$ and 40) alloys attracted much attention from a quiet different viewpoint. Fukuhara *et al.* found strange behavior of the electrical conductivity for the amorphous $(\text{Ni}_{0.6}\text{Nb}_{0.4})_{100-x}\text{Zr}_x\text{H}_y$ ($x=30, 40$ and $y=9-11$) alloys such as the Coulomb oscillation [4]. Oji *et al.* measured XAFS spectra for the amorphous $(\text{Ni}_{0.6}\text{Nb}_{0.4})_{100-x}\text{Zr}_x$ ($x=30, 40$) alloys and their hydrogenated $(\text{Ni}_{0.6}\text{Nb}_{0.4})_{100-x}\text{Zr}_x\text{H}_y$ ($x=30, 40$ and $y=9$ and 11) ones [5]. They achieved curve fitting analysis for the XAFS results of the Nb and Zr K-edges, (not for the Ni K-edge) and estimated lattice parameters for these amorphous alloys and their hydrogenated one.

In order to elucidate the structural origin of the strange electrical behaviors for these hydrogenated amorphous alloys, it is necessary to obtain more detail structure information; concentration dependence of the local structures of the $x=30, 35$ and 40 for $(\text{Ni}_{0.6}\text{Nb}_{0.4})_{100-x}\text{Zr}_x$ amorphous alloys and fitting analysis for the Ni K-edge XAFS data as well as the Nb and Zr K-edges. In the present work XAFS measurements for the $(\text{Ni}_{0.6}\text{Nb}_{0.4})_{100-x}\text{Zr}_x$ ($x=30, 35$ and 40) alloys were carried out and the results were compared with the first principle calculation based on the icosahedral cluster model.

2. Experiments

Ribbon samples were prepared by a melt-quenching technique using a single-roller apparatus. XAFS measurements of the Ni, Nb and Zr K-edges were made at 20K in a transmission mode at beam line BL14B2 of the large scale synchrotron radiation facility, SPring-8, in Hyogo, Japan. The incident X-ray was monochromatized by a Si double crystal monochromator: Si(311) plane for

the Zr and Nb K-edges and Si(111) for the Ni K-edge. The higher harmonics of the incident X-ray were reduced by two Rh-coated mirrors. The XAFS data were analyzed using coded program *Athena*.

3. Results and discussion

Figure 1 shows the results of the XAFS oscillations $\chi(k)$ weighted by k^3 of the Ni-Kedges for the amorphous $(\text{Ni}_{0.6}\text{Nb}_{0.4})_{100-x}\text{Zr}_x$ ($x=30, 35$ and 40) alloys. **Figure 2** shows the results of the Fourier transform $|F(r)|$ of $k^3 \cdot \chi(k)$ of the Ni K-edge for amorphous $(\text{Ni}_{0.6}\text{Nb}_{0.4})_{100-x}\text{Zr}_x$ ($x=30, 35$ and 40) alloys. The k -range in the Fourier transform is $2 < k < 12 (\text{\AA}^{-1})$. The Fourier transforms of the Nb and Zr K-edges are shown in **Fig. 3** and **4**, respectively with the same k -range as for the Ni K-edge.

The characteristic features of the XAFS results are that the $|F(r)|$ curves of the three elements do not change continuously with Zr concentration but change sharply from $x=30$ to 35 . This indicates that the local structures of the amorphous $(\text{Ni}_{0.6}\text{Nb}_{0.4})_{100-x}\text{Zr}_x$ alloys of $x < 35$ are different from those of $x > 35$. The second feature of the XAFS results is that the first peak of the $|F(r)|$ for the Ni K-edge clearly splits into two while those for the Nb and Zr ones show a single peak.

Considering atomic radii of the constituent elements, i. e. $r_{\text{Ni}}=1.24$, $r_{\text{Nb}}=1.47$ and $r_{\text{Zr}}=1.60$ (in \AA), the nearest neighbor peak of the $|F(r)|$ for the Ni K-edge consists of Ni-

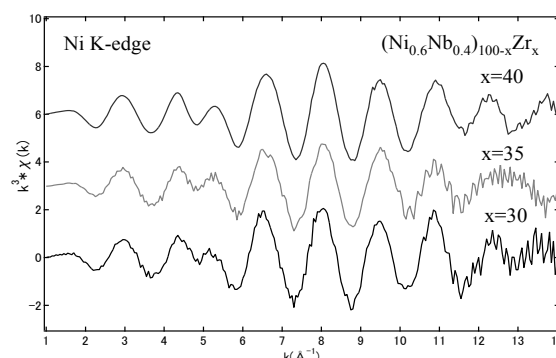


Fig.1 XAFS oscillation $\chi(k) \cdot k^3$ of the Ni K-edge for amorphous $(\text{Ni}_{0.6}\text{Nb}_{0.4})_{100-x}\text{Zr}_x$ ($x=30, 35$ and 40) alloys at 20K.

[†] Received on 30 September 2010

* Institute for Materials Research, Tohoku University, 2-1-1 Katahira, Aoba, Sendai 980-8577, Japan

** National College of Technology-Sendai, 48 Nodayama, Shiote-Aza, Natori 981-1239, Japan

*** Faculty of Engineering, Shizuoka University, Hamamatsu 432-8561, Japan

**** Tohoku University, 2-1-1 Katahira, Aoba, Sendai 980-8577 Japan

Transactions of JWRI is published by Joining and Welding Research Institute, Osaka University, Ibaraki, Osaka 567-0047, Japan

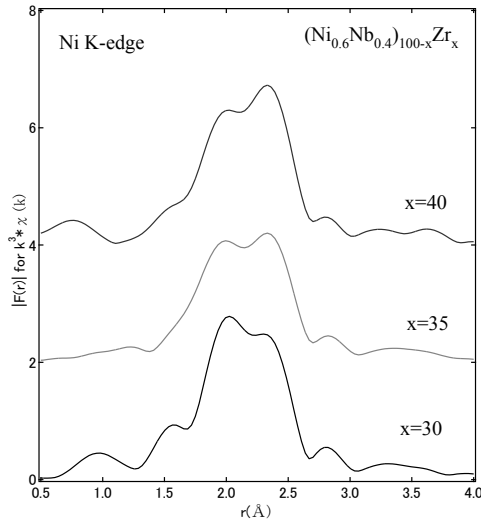


Fig.2 Fourier transform of the Ni K-edge of $k^3 \cdot \chi(k)$ for the amorphous $(\text{Ni}_{0.6}\text{Nb}_{0.4})_{100-x}\text{Zr}_x$ ($x=30, 35$ and 40) alloys at 20K.

Ni correlations and the second one Ni-Nb and Ni-Zr ones. This can be proved by the fact that the intensity of the first shoulder in the $|F(r)|$ decreases with increase in Zr concentration. On the contrary, the intensity of the second one increases with Zr as shown in Fig. 1. A broad single peak of $|F(r)|$ for the Nb and Zr K-edges may consist of mainly Nb-Ni and Zr-Ni correlations and a small number of Nb-Nb(Zr) and Zr-Zr(Nb) ones. One of the authors, N. Fujima, calculated electronic states of the icosahedral $\text{Ni}_5\text{Nb}_3\text{Zr}_5$ clusters and optimized structures by using the first principles calculation. The results of the calculation suggest that Ni-centered icosahedral clusters are most stable among three types of a centered atom (Ni, Nb and Zr). There are two types of energetically stable icosahedrons, i.e. distorted one(*d-icosa*) and isotropic one(*i-icosa*). The *d-icosa* exhibits similar atomic configuration as the $\text{NiZr}(\text{C}33)$ and $\text{NiZr}_2(\text{C}16)$ crystalline compounds. Fourier transforms $|F(r)|$'s are calculated for the two Ni-centered icosahedral clusters, *d-icosa* and *i-icosa*, using the coded program Artemis. $|F(r)|$ result of the Ni K-edge for *i-icosa* shows a single broad peak while *d-icosa* shows a tendency of splitting. Though further elaborated works are necessary, a distorted icosahedron with a similar local structure as Ni-Zr compounds is a favorable structural model for the $(\text{Ni}_{0.6}\text{Nb}_{0.4})_{65}\text{Zr}_{35}$ amorphous alloy.

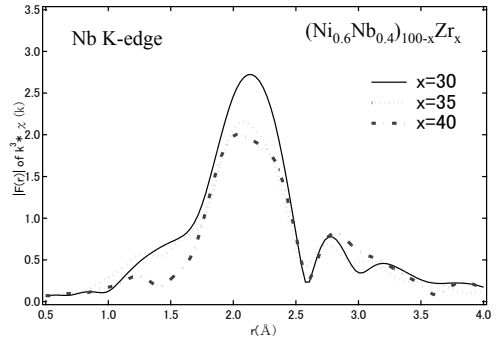


Fig.3 Fourier transform of the Nb K-edge of $k^3 \cdot \chi(k)$ for the amorphous $(\text{Ni}_{0.6}\text{Nb}_{0.4})_{100-x}\text{Zr}_x$ ($x=30, 35$ and 40) alloys at 20K.

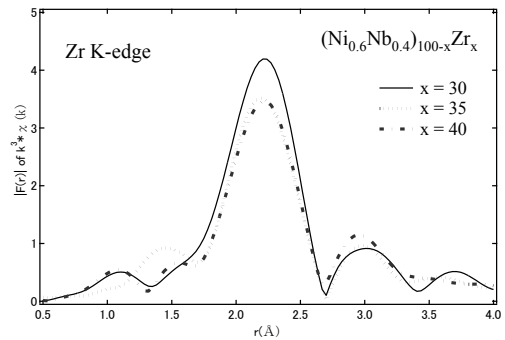


Fig.4 Fourier transform of the Zr K-edge of $k^3 \cdot \chi(k)$ for the amorphous $(\text{Ni}_{0.6}\text{Nb}_{0.4})_{100-x}\text{Zr}_x$ ($x=30, 35$ and 40) alloys at 20K.

References

- [1] H. Kimura, A. Inoue, S. Yamaura, K. Sasamori, M. Nishida, Y. Shimpo and H. Okouchi: Mater. Trans., 44 (2003), pp.1167-1171.
- [2] S. Yamaura, M. Sakurai, M. Hasegawa, K. Wakoh, Y. Shimpo, M. Nishida, H. Kimura, E. Matsubara and A. Inoue: Acta Mater., 53 (2005), pp.3703-3711.
- [3] M. Sakurai, S. Yamaura, K. Wakoh, E. Matsubara and A. Inoue: J. Metastable and Nanocryst., 24-25 (2005), pp.551-554.
- [4] M. Fukuhara and A. Inoue: J. Appl. Phys., 105 (2009), pp.63715-63719.
- [5] H. Oji, K. Handa, J. Ide, T. Honma, S. Yamaura, A. Inoue, N. Umesaki, S. Emura and M. Fukuhara: J. Appl. Phys., 105 (2009), pp.113527-113533.